Infrared Photodissociation Spectroscopy of Mass-Selected $Al^+(CO_2)_n$ and $Al^+(CO_2)_nAr$ Clusters

R. S. Walters, N. R. Brinkmann, H. F. Schaefer, and M. A. Duncan*

Department of Chemistry, University of Georgia, Athens, Georgia 30602-2556

Received: April 22, 2003; In Final Form: July 10, 2003

Weakly bound $Al^+(CO_2)_n$ and $Al^+(CO_2)_nAr$ complexes are produced by laser vaporization in a pulsed supersonic expansion. The clusters are mass-selected and studied by laser photodissociation spectroscopy in a reflectron time-of-flight mass spectrometer. The excitation laser is an OPO/OPA system that produces tunable infrared light near the asymmetric stretch of CO_2. $Al^+(CO_2)_n$ clusters fragment by the loss of CO_2, while $Al^+(CO_2)_n$-Ar clusters fragment by the loss of argon. Dissociation is more efficient on resonance, and thus monitoring the fragmentation as a function of wavelength produces the infrared resonance-enhanced photodissociation (IR−REPD) spectrum of the complex of interest. The spectra show a blue-shift of the asymmetric CO_2 stretch which decreases as the size of the cluster increases. $Al^+(CO_2)_nAr$ transitions appear at essentially the same frequencies as those for the pure CO_2 analogues but with significantly narrower line widths. The observed infrared bands are compared to the predictions of theory and specific structures are proposed for the smaller clusters. Band positions in the larger clusters provide insight into the effects of solvation.

Introduction

Metal-ion complexes that are produced and studied in the gas phase provide models to explore ion solvation and metal−ligand bonding.[1−3] Theory has investigated these systems,[4−9] but direct comparisons to experimental measurements are sometimes problematic. Various mass spectrometry measurements have probed the binding energetics and reactivities of metal ion complexes.[10−16] Electronic spectroscopy has provided information on excited states,[17−23] but these are often difficult to treat with theory. Detailed information on these complexes in their ground states is essential for meaningful comparisons to theory. Recent advances in high-resolution photoelectron spectroscopy[24−26] and particularly in IR photodissociation spectroscopy[27−33] are beginning to provide new insights into the structures and characteristics of these metal-ion complexes. In the present work, we report infrared resonance enhanced photodissociation (IR-REPD) spectroscopy for mass-selected $Al^+(CO_2)_n$ and $Al^+(CO_2)_nAr$ clusters. This study provides the first structural information for these complexes in their electronic ground states.

Its simple electronic structure makes aluminum attractive for both theory and experimental cluster studies. Thus, many groups have performed calculations on neutral[4,34−38] and ionized[4,8,9,11] complexes of aluminum with various small molecules. The aluminum atom has accessible low-energy electronic states and these have been exploited to study van der Waals complexes of the form Al-L_x.[24,39,40] Also, the first ionization potential (IP) of aluminum is relatively low (5.986 eV) and this is accessible with tunable UV lasers. Therefore, the IPs of complexes with small molecules have been measured,[39,41,42] and ZEKE photoelectron spectroscopy has been performed on several aluminum complexes.[24,26] Our lab observed solvation-induced metal oxidation reactions in threshold ionization measurements on Al−$(CO_2)_n$.[42] Because the cation is closed-shelled ($3s^2$), clusters containing Al^+ do not have low-lying electronic states that are easily accessible by tunable laser sources. Thus, electronic spectroscopy is problematic for $Al^+(L)_n$ complexes. Dagdigian used vacuum UV generation to acquire the electronic spectra of Al^+−Ar by laser-induced fluorescence,[43] and Kleiber employed similar methods to study $Al^+(C_2H_4)$ via photodissociation spectroscopy.[44] Although spectroscopy is limited, many groups have studied aluminum cation complexes to probe cluster reactions. Bowers explored the possibility of Al^+ insertion into H_2 by equilibrium mass spectrometry and ab initio studies.[13] Bondybey and co-workers have investigated solvation processes in larger aluminum ion complexes.[15] Because of the interesting chemistry found in these systems, aluminum complexes continue to be targets for spectroscopic studies. Infrared spectroscopic techniques are not likely to induce photochemistry and are therefore useful to probe the ground states of these cation complexes. We have recently reported a study of the infrared spectroscopy of $Mg^+(CO_2)_n$ complexes,[29] and this study of Al^+ complexes provides a comparison to those results.

Infrared spectroscopy is an established method for inorganic and organometallic complexes in the condensed phase.[45] Unfortunately, IR measurements on gas phase metal ion complexes suffer from low sample density, requiring intense light sources that are not generally available. However, recent advances in IR optical parametric oscillator (OPO) systems have opened the door for infrared measurements on low density ions via photodissociation. The infrared predissociation of alkali-metal cation complexes has been studied extensively by Lisy and co-workers for a number of different ligands.[27] Recently, our lab produced the first IR photodissociation spectra for transition-metal cation complexes in a study on $Fe^+(CO_2)_n$ complexes.[28] More recent experiments have extended the work to other metal ions (e.g., Mg^+) and other ligands.[29,30] Our group and others have also employed the tunable infrared radiation available from a free electron laser to do similar IR photodissociation studies on more strongly bound organometallic complexes.[31,33] We continue this kind of work in the present

* To whom correspondence should be addressed. E-mail: maduncan@uga.edu.

10.1021/jp030491k CCC: $25.00
Published on Web 08/27/2003

study with $Al^+(CO_2)_n$ for comparison to our previous studies on $Fe^+(CO_2)_n$ and $Mg^+(CO_2)_n$.[28,29] IR−REPD spectroscopy of mass-selected $Al^+(CO_2)_n$ ($n = 1-11$) and $Al^+(CO_2)_nAr$ ($n = 1-3$) clusters is reported. Detailed vibrational spectra are obtained from enhanced infrared photodissociation near the ν_3 of free CO_2, and spectral features are compared to frequency calculations for theoretical structures.

Experimental Section

Clusters for these experiments are produced by laser vaporization in a pulsed supersonic expansion and mass analyzed in a reflectron time-of-flight mass-spectrometer (TOF-MS). The molecular beam apparatus and the mass-spectrometer have been described previously.[23,32] The third harmonic of a Nd:YAG (355 nm) is used to vaporize a rotating aluminum rod. Ionized $Al^+(CO_2)_n$ and $Al^+(CO_2)_nAr$ clusters are produced directly from the laser vaporization process in expansions of pure CO_2 or CO_2 seeded in argon using a pulsed General Valve (1 mm nozzle) at 40 psi backing pressure and a 200 μsec pulse duration. The free expansion is skimmed from the source chamber into the mass-spectrometer and the ions are extracted into the first drift region of the reflectron using pulsed acceleration voltages. They are then mass-selected by pulsed deflection plates before entering the reflectron where they are dissociated at the turning point by the infrared output of an optical parametric oscillator/amplifier (OPO/OPA). Parent and daughter ions are mass-analyzed in the second flight tube and mass spectra are recorded with a digital oscilloscope (LeCroy 9310). The data are transferred to a PC via an IEEE interface. Infrared resonance enhanced photodissociation (IR-REPD) spectra are obtained by monitoring the intensity of the fragment ions as a function of wavelength.[28−30]

An IR OPO/OPA (Laser Vision) pumped by a Continuum 8010 Nd:YAG is used for photodissociation. This system has two 532 nm-pumped KTP crystals in the grating tuned oscillator section and four KTA crystals in the amplifier section. The signal output from the oscillator is combined with residual 1064 nm in the amplifier, and difference frequency generation here provides the tunable near-IR output from 2.2 to 4.9 μm (4500 to 2050 cm^{-1}). In this experiment, the OPO is unfocused to prevent power broadening. Near 2350 cm^{-1}, the laser pulse energies range from 1 to 3 mJ/pulse with an approximate line width of 0.3 cm^{-1}. Typical spectra are obtained at ~1.2 cm^{-1} steps and averaged over 250 laser shots.

The DFT quantum chemical computations were performed on $Al^+CO_2(_n)$, where $n = 0$, 1, 2, and 3, using the GAUSSIAN 94 program package.[46] Two gradient-corrected functionals, denoted B3LYP and BP86, were used to compute the geometries, energies, and harmonic vibrational frequencies. Energies were converged to at least 10^{-6} hartrees in the self-consistent field procedures, although the absolute accuracy may be somewhat lower due to numerical integration procedures. The B3LYP functional is a hybrid Hartree−Fock and density functional theory (HF/DFT) method using Becke's three-parameter exchange functional (B3)[47] with the Lee, Yang, and Parr correlation functional (LYP).[48] The BP86 functional uses Becke's 1988 exchange functional (B)[49] and the 1986 correlation correction of Perdew (P86).[50]

We employed a double-ζ basis set with polarization functions, denoted DZP. This basis was constructed from the Huzinaga−Dunning[51,52] set of contracted double-ζ Gaussian functions. Added to this was one set of five *d*-type polarization functions for each Al, C, and O atom [$\alpha_d(Al) = 0.325$, $\alpha_d(C) = 0.750$, and $\alpha_d(O) = 0.850$]. The final contraction scheme for this basis is Al(12*s*8*p*1*d*/6*s*4*p*1*d*) and C,O(9*s*5*p*1*d*/4*s*2*p*1*d*). Geometries were optimized for each molecular species with each functional using analytic gradient techniques. Residual Cartesian gradients were less than 1.5×10^{-5} hartree/Bohr. Stationary points found in optimizations were confirmed as minima by computing the harmonic vibrational frequencies using analytic second derivatives with each functional.

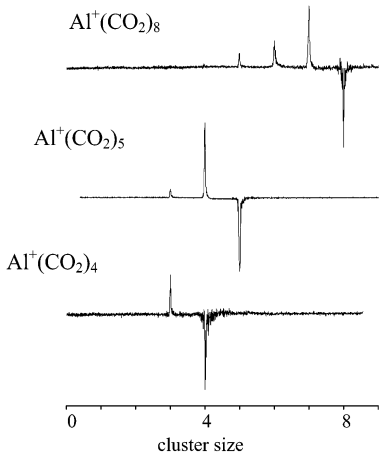

Figure 1. Infrared photodissociation mass spectra of $Al^+(CO_2)_n$ ($n =$ 4,5,8) complexes at 2349 cm^{-1} using low laser power. The various complexes all fragment by the loss of intact CO_2 molecules.

Results and Discussion

The mass distribution of clusters produced by laser vaporization of aluminum in a pure CO_2 expansion is typical of that we reported previously.[42] It is composed of a smooth progression of mass peaks that are assigned to $Al^+(CO_2)_n$ complexes, where $n \sim 0-20$. The intensities drop by a factor of about two after $n = 11$, and we are therefore not able to study clusters larger than this. There is no evidence in the mass spectrum for metal-oxides or metal-carbides produced from reactions in the source, and there are no peaks that stand out as so-called magic numbers.

Examples of the photodissociation mass spectra for various $Al^+(CO_2)_n$ complexes are shown in Figure 1. To obtain these, each complex is mass-selected from the source distribution and the infrared laser is adjusted in space and time to intersect the ions in the turning region of the reflectron. Mass spectra are recorded both with and without the photodissociation laser to produce these difference spectra. The negative peaks correspond to the depletion of the parent ion, whereas the positive peaks indicate the appearance of the photofragments produced by IR photodissociation. Here, each of the smaller $Al^+(CO_2)_n$ complexes fragment by the loss of one or two CO_2 molecules with the output of the OPO laser tuned near the 2349 cm^{-1} resonance characteristic of the CO_2 asymmetric stretch. The larger clusters (e.g., $n = 8$) fragment more efficiently and lose more CO_2 units on average for the same excitation laser conditions. As shown, there is no strong preference for any particular cluster size that might indicate the presence of a closed coordination sphere around the metal ion. Photodissociation of the $Al^+(CO_2)_2$ cluster (not shown) is quite difficult, leading to the loss of only one CO_2 molecule. The dissociation efficiency increases by a factor of 4−5 in going to the next-larger $n = 3$ species. Photodissociation of the $n = 1$ complex is not observed even at the highest laser fluence. The difficulty in fragmenting these smallest complexes was also found previously for $Fe^+(CO_2)_n$, $Mg^+(CO_2)_n$ and $Ni^+(C_2H_2)_n$ systems.[28−30]

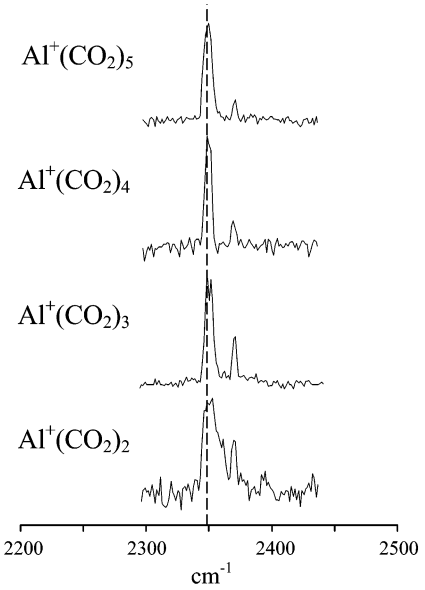

Figure 2. Wavelength dependence of the infrared photodissociation of $Al^+(CO_2)_n$ clusters in the small size range measured in the n-1 mass channel. The smallest complex ($n = 1$) cannot be fragmented, but the dissociation efficiency increases for larger clusters.

As we have discussed before,[28−30] the low fragmentation yields for the smaller complexes are due to their relatively higher bond strengths and their low vibrational density of states. For photodissociation to occur, the molecule must absorb energy greater than the strength of its weakest bond and the vibrational frequencies here may not correspond to enough energy to do this. If the bond energy is higher than the energy of one photon, then multiphoton absorption is necessary, the efficiency of which increases as the density of states increases. Anharmonicity in the higher levels of the mode excited initially lead to a loss of resonance in this coordinate, and other vibrational states are required to maintain resonance in a multiphoton absorption process. Fragmentation also requires that the excited coordinate (asymmetric CO_2 stretch) couple with the dissociation coordinate (metal−ligand stretch) via intramolecular vibrational relaxation (IVR), the rate of which also increases as state densities increase. Small clusters are expected to have relatively high binding energies and a low density of states. Theoretical calculations on the binding energy of Al^+-CO_2 range from 10 to 20 kcal/mol (3500−7000 cm^{-1}),[11] and therefore a multiphoton process is definitely needed to achieve dissociation in the $n = 1$ complex when the CO_2 asymmetric stretch (2349 cm^{-1} in free CO_2) is excited. Larger clusters are expected to have much weaker bond strengths when the second solvation layer forms. The CO_2 dimer has a bond strength of about 485 cm^{-1}.[53] Therefore, when CO_2 is not directly attached to the metal ion, its binding should have energies near this value and absorption of one photon could induce dissociation. Furthermore, the vibrational state density increases with an increase in cluster size, improving both multiphoton absorption and IVR. It is therefore understandable that the small clusters ($n = 1,2$) have low dissociation yields and that the dissociation of larger complexes is gradually more efficient. In some complexes we have studied, e.g., $Ni^+(C_2H_2)_n$[30] or $Ni^+(CO_2)_n$,[54] there is a sharp change in dissociation efficiency at a cluster size just beyond a filled coordination shell. However, the change in dissociation yield is more gradual here.

Figure 2 shows that the photodissociation yield in these $Al^+(CO_2)_n$ complexes is wavelength dependent. The position of the asymmetric stretch in isolated CO_2 (2349 cm^{-1}) is indicated in the figure with a vertical dashed line. As shown, each of these complexes has a resonance enhancement in its photodissociation yield that occurs near this "free CO_2" frequency. Each of the complexes has a resonance (7−12 cm^{-1} fwhm) either at or just to the blue of the free CO_2 resonance, with a weaker band shifted about 25 cm^{-1} to the blue from this. The signal level for the $n = 2$ complex is poor, consistent with its inefficient photodissociation, as discussed above. The signal levels are improved and the lines are somewhat sharper for the larger complexes, consistent with their improved dissociation efficiencies.

The observation of a resonance near the value of the free-CO_2 asymmetric stretch establishes that these clusters are weakly bound complexes with intact CO_2 molecules present. No other resonances are observed within the region of 2050−3000 cm^{-1}. If an insertion reaction with CO_2 occurred, an oxide-carbonyl species, e.g., $OC-AlO^+(CO_2)_{n-1}$ would have the same mass as the corresponding $Al^+(CO_2)_n$ species and could not be distinguished by mass spectrometry. However, such an inserted species would likely have a carbonyl resonance at lower frequency in the 2000−2200 region, and no such peaks are observed. The spectra are therefore consistent with complexes having only intact CO_2 molecules clustering with Al^+.

The IR spectra of these complexes can be used to obtain information about their structures. In the previous work on metal ion−CO_2 complexes, the primary bonding motif involved a linear M^+-OCO structure for the $n = 1$ complexes, resulting from the charge-quadrupole electrostatic interaction.[28,29] Both theory and experiment agreed on this structure for the Mg^+-CO_2 and Fe^+CO_2 $n = 1$ complexes, and the same kind of near-linear M^+-OCO configuration was the basis for the structures of multi-ligand complexes. A similar bonding configuration is also likely here. In the previous systems, the linear M^+-OCO configuration led to asymmetric stretch resonances that were shifted to higher frequency in the complexes compared to this frequency in the free CO_2 molecule (2349 cm^{-1}). Blue shifts of 20−30 cm^{-1} were seen before. The spectra here have structure both at the frequency of the free molecule and some to the blue of this. However, the $n = 2$ spectrum is broad and the $n = 3$ spectrum has a closely spaced doublet near the free CO_2 value. The $n = 4$ and 5 species have the small peak to the blue and a larger peak that is centered near the free-CO_2 value. On first glance then, the data here could be consistent with structures based on the same kind of linear M^+-OCO configurations seen previously, but better quality spectra would be desirable. It would also be valuable to know what structures are predicted by theory and what IR spectra are expected for these.

We have therefore investigated the three smallest complexes with density functional theory to determine calculated structures and vibrational spectra. The level of theory employed here is comparable to that which we employed previously for corresponding $Mg^+(CO_2)_n$ complexes.[29] For each complex, we investigated several possible binding configurations. We explored the most likely ground state for the system that has a singlet electronic configuration for the Al^+, and we also examined the first excited triplet configuration. We also performed calculations at the same levels for the free aluminum cation and for the free CO_2 molecule. The various structures and energetics for these systems are given in Table 1.

As shown in the table, stable bound configurations are found for each cluster size for both the ground state singlets and triplets. The triplet states have open shell configurations, and give rise to more strongly bound complexes, but the singlet states still lie at lower energy and are therefore the ground states for each complex. These various minimum energy structures are

TABLE 1: Total Electronic Energies (hartrees) of Al^+, CO_2, Al^+CO_2, and $Al^+(CO_2)_2$ Minima with a DZP Basis Set.

system	B3LYP	D_e (kcal/mol)	BP86	D_e (kcal/mol)
Al^+ (singlet)	−242.15186		−242.14321	
	(−242.15186)		(−242.14321)	
Al^+ (triplet)	−241.97484		−241.97203	
	(−241.97484)		(−241.97203)	
CO_2	−188.62082		−188.63002	
	(−188.60916)		(−188.61878)	
Al^+CO_2 ($C_{\infty v}$, triplet)	−430.65228	35.5	−430.66034	36.6
	(−430.63967)	(34.9)	(−430.64854)	(36.2)
Al^+CO_2 ($C_{\infty v}$, singlet)	−430.79247	12.4	−430.79404	13.1
	(−430.78021)	(12.1)	(−430.78222)	(12.7)
Al^+CO_2 (C_{2v}, triplet)	−430.67110	47.3	−430.67550	46.1
	(−430.65984)	(47.6)	(−430.66477)	(46.4)
$Al^+(CO_2)_2$ (D_{2d}, triplet)	−619.31910	64.4	−619.33099	62.1
	(−619.29464)	(63.7)	(−619.30760)	(61.5)
$Al^+(CO_2)_2$ (C_{2v}, triplet)	−619.31231	60.1	−619.33010	62.1
	(−619.28738)	(59.1)	(619.30763)	(61.5)
$Al^+(CO_2)_2$ (C_{2v}, singlet)	−619.42619	20.5	−619.43727	21.4
	(−619.40174)	(19.8)	(619.41365)	(20.6)
$Al^+(CO_2)_2$ (C_{2v}, triplet) "dimer"	−619.23985	14.7	−619.26539	20.9
	(−619.21351)	(12.8)	(−619.24028)	(19.3)
$Al^+(CO_2)_2$ (C_{2v}, singlet) "dimer"	−619.36089	20.5	−619.37770	16.0
	(−619.33409)	(22.6)	(619.35215)	(18.0)
$Al^+(CO_2)_3$ (C_s, triplet)	−807.95086	71.3	−807.97975	78.8
	(−807.19344)	(69.7)	(−807.94435)	(72.8)
$Al^+(CO_2)_3$ (C_{2v}, triplet)	−807.95086	71.3		
	(−807.91344)	(69.7)		
$Al^+(CO_2)_3$ (C_{3v}, singlet)	−808.05693	26.7	−808.07691	27.4
	(−808.02042)	(25.8)	(−808.04159)	(26.4)

Zero-point corrected values are listed in parentheses. D_e values are in kcal/mol.

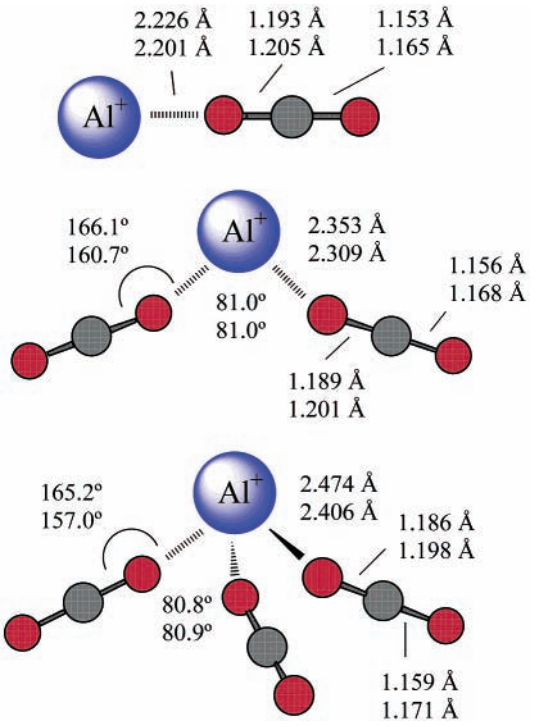

Figure 3. Theoretically predicted structures for the $Al^+(CO_2)_n$ complexes ($n = 1,2,3$). The structural parameters indicated are for the B3LYP (upper numbers) and BP86 functionals. The symmetries are $C_{\infty v}$, C_{2v}, and C_{3v} respectively.

shown in detail in Figure 3. The $n = 1$ complex has its lowest energy in the linear $C_{\infty v}$ configuration as expected for the charge-quadrupole electrostatic interaction. This is completely consistent with our expectations for this complex based on previous experiments and theory on other $M^+(CO_2)$ complexes.[28,29] A local minimum is found in the C_{2v} configuration for the triplet species, but not for the singlet. The $n = 2$ species has a lowest energy C_{2v} configuration with both CO_2 molecules bound end-on to the metal ion and separated by an angle of about 81°. A second less stable local minimum is found that also has C_{2v} symmetry, but with only one CO_2 bound to the metal. The second CO_2 is bound to the first in a so-called "dimer" configuration, with both CO_2 molecules distorted from linearity. As found previously for $Mg^+(CO_2)_2$, the all-linear configuration with both CO_2 molecules attached to metal is not a minimum.[29] The CO_2 ligands prefer instead to bind more on the same side of the metal. This observation was explained initially by Bauschlicher to arise from the high polarizability of the Mg^+ $3s^1$ electron.[4] When the first CO_2 binds to the cation, this valence electron cloud is polarized and a lobe of negative charge is induced on the backside of the metal. The second ligand avoids this negative region and binds on the same side as the first. The observation of this same structure here suggests that the same polarization effect occurs for the Al^+ $3s^2$ valence electron cloud. The $n = 3$ complex continues this structural pattern, with all three CO_2 molecules binding end-on to the cation, but on the same side of it in a C_{3v} structure. This same structure was also found in our previous study of $Mg^+(CO_2)_3$, where it was also explained to arise from the polarization of the valence electron cloud on the metal.[29] Again, the aluminum cation follows the same binding pattern as magnesium cation, with same-side ligand attachment.

As shown in the figure, there is a slight distortion of the CO_2 molecules in each of these clusters, so that the C−O bond nearest the metal is elongated compared to the opposite one. We have seen this same effect in our previous study of $Mg^+(CO_2)_n$ clusters,[29] and it was also reported earlier by Bauschlicher in his original work on $Mg^+(CO_2)_n$ complexes.[4] This behavior is consistent with the recently discussed *bond activation-reinforcement* (BAR) rule,[55] that predicts when bonds will be distorted based on the electronegativities of the adjacent atoms. The oxygen where binding occurs is more electronegative

than carbon, and so electron density is removed from the C−O bond adjacent to the metal, resulting in its slight elongation.

The calculated binding energies of the outermost ligands in these complexes decrease with cluster size. The binding energies shown in Table 1 are total energies for the binding of all ligands, while the incremental binding for the outer ligand is more relevant for photodissociation. These binding energies are $n =$ 1: 12.1 kcal/mol (4230 cm^{-1}), $n = 2$: 7.7 kcal/mol (2690 cm^{-1}) and $n = 3$: 6.0 kcal/mol (2100 cm^{-1}). Therefore, the binding energy of the last ligand decreases as cluster size increases. According to these calculations, photodissociation requires at least two photons for the $n = 1,2$ complexes, but is a one-photon process for the $n = 3$ complex. This is completely consistent with the sudden increase in the photodissociation yield that we see for the $n = 3$ species. Presumably the larger complexes would also have low enough binding energies so that one-photon dissociation is possible.

To compare the calculated structures with our infrared spectra, we have calculated the vibrations for these lowest energy structures, and these are presented in Table 2. To achieve a fair comparison with experiment, we have calculated the vibrations of isolated CO_2 at the same level of theory. As expected, the computed harmonic frequencies differ systematically from the well-known experimental values. In particular, the ν_3 asymmetric stretch is calculated using either of the two functionals to be higher than the experimental value. We therefore focus on just the asymmetric stretch, and shift the various frequencies for each of the complexes by an amount necessary to bring the values for free CO_2 into agreement with experiment. The downward shift is 90 cm^{-1} for B3LYP and 26 cm^{-1} for BP86. These shifted values are also shown in Table 2, where they are compared to the experimental values discussed below.

To obtain vibrational spectra for the $n = 1$ complex which could not be dissociated and to obtain higher quality spectra for the other small complexes, we use the method of rare gas "tagging." As shown previously by our group and by several others in ion photodissociation spectroscopy, this technique makes it possible to overcome low fragmentation yields by attaching weakly bound rare gas atoms (i.e., argon) to otherwise strongly bound clusters.[28,29,56−60] The charge-induced dipole interaction between the argon and the metal ion results in a lower binding energy (e.g., ∼980 cm^{-1} for Al^+Ar)[39] than the metal-CO_2 bonding, and such mixed clusters have higher vibrational state densities. Thus, the "tagged" complexes fragment by the loss of argon and are easier to photodissociate than the pure CO_2 clusters. Attaching argon usually results in a weak perturbation on the complex, causing little or no spectral shift in its vibrational spectrum. We are able to form the mixed CO_2/Ar complexes here only for the small cluster sizes ($n = 1-3$). Photodissociation of these complexes proceeds by the elimination of argon, as expected, and we are able to measure vibrational spectra for each of the $n = 1,2,3$ species in this way.

Figure 4 shows the IR−REPD spectra of $Al^+(CO_2)_2$ and $Al^+(CO_2)_2Ar$ from 2300 to 2420 cm^{-1} for comparison. The spectra are obtained for the pure CO_2 and the mixed clusters by monitoring the $Al^+(CO_2)$ and $Al^+(CO_2)_2$ fragment mass channels, respectively. Two resonances are observed at about 3 and 20 cm^{-1} to the blue of ν_3 in free CO_2. No significant spectral shift is observed for the argon-tagged complex while the line width is narrowed from 11 to 5 cm^{-1} fwhm. Both the pure and mixed species are thought to be cold due to the known properties of the source. The mixed cluster has a lower binding energy and a greater vibrational state density, and we conclude that the narrower line width results because the argon complex dissociates via a single photon process. Lower laser power is required and the power broadening seen for the neat complex is reduced. Similar results are obtained when comparing the spectra of $Al^+(CO_2)_3$ and $Al^+(CO_2)_3Ar$.

Figure 5 shows the photodissociation spectra for $Al^+(CO_2)_{1-3}Ar$ at low laser power. Strong features are observed to the blue of the asymmetric stretch of free CO_2 (dotted line), and the

TABLE 2: Theoretical Harmonic Vibrational Frequencies in cm^{-1} for the Lowest Energy Singlet States of CO_2, Al^+CO_2, $Al^+(CO_2)_2$, and $Al^+(CO_2)_3$ with a DZP Basis Set[a]

	B3LYP	BP86	expt
	CO_2		
ω_1 (Σ_g)	1363 (0)	1308 (0)	1333
ω_2 (Π_u)	660 (30)	627 (21)	667
ω_3 (Σ_u)	2439 (652)	2375 (530)	2349
	$Al^+(CO_2)$ ($C_{\infty v}$, singlet)		
ω_1 (Σ)	2457 (925)	2389 (752)	
ω_1 (Σ) (corrected)	2367	2363	2366
ω_2	1353 (109)	1300 (99)	
ω_3	175 (154)	192 (153)	
ω_4 (Π)	637 (37)	602 (29)	
ω_5	637 (27)	602 (29)	
ω_6	61 (2)	51 (2)	
ω_7	61 (2)	51 (2)	
	$Al^+(CO_2)_2$ (C_{2v}, singlet)		
ω_1 (A_1) (in-phase)	2461 (619)	2392 (399)	
ω_1 (A_1) (corrected)	2371	2366	2369
ω_2	1359 (52)	1304 (38)	
ω_3	641 (40)	603 (29)	
ω_4	174 (116)	195 (113)	
ω_5	62 (3)	62 (2)	
ω_5	28 (1)	28 (1)	
ω_7 (A_2)	642 (0)	606 (3)	
ω_8	60 (0)	54 (0)	
ω_9 (B_1)	644 (68)	607 (51)	
ω_{10}	62 (2)	52 (1)	
ω_{11} (B_2) (out-of-phase)	2443 (1356)	2377 (1273)	
ω_{11} (B_2) (corrected)	2353	2351	2352
ω_{12}	1357 (88)	1302 (85)	
ω_{13}	638 (25)	601 (16)	
ω_{14}	119 (98)	141 (105)	
ω_{15}	44 (1)	46 (0.2)	
	$Al^+(CO_2)_3$ (C_{3v}, singlet)		
ω_1 (A′) (in-phase)	2465 (504)	2395 (232)	
ω_1 (A′) (corrected)	2375	2369	2371
ω_2 (out-of-phase)	2442 (1224)	2375 (1183)	
ω_2 (corrected)	2352	2349	2351
ω_3	1362 (31)	1305 (19)	
ω_4	1360 (54)	1304 (53)	
ω_5	646 (54)	609 (31)	
ω_5	645 (59)	606 (47)	
ω_7	642 (16)	605 (11)	
ω_8	173 (91)	195 (88)	
ω_9	100 (60)	121 (72)	
ω_{10}	60 (5)	63 (2)	
ω_{11}	56 (5)	57 (3)	
ω_{12}	40 (3)	43 (1)	
ω_{13}	27 (1)	29 (1)	
ω_{14}	20 (0.3)	20 (0.6)	
ω_{15} (A″) (out-of-phase)	2442 (1242)	2375 (1156)	
ω_{15} (A″) (corrected)	2352	2349	2351
ω_{16}	1360 (55)	1303 (52)	
ω_{17}	646 (31)	609 (36)	
ω_{18}	642 (27)	606 (0.1)	
ω_{19}	642 (0.2)	605 (5)	
ω_{20}	102 (61)	122 (73)	
ω_{21}	61 (6)	62 (2)	
ω_{22}	39 (3)	44(2)	
ω_{23}	35 (0.1)	31 (0)	
ω_{24}	20 (0.6)	20 (0.6)	

[a] Experimental fundamental vibrational frequencies are in cm^{-1}. Computed IR intensities (km/mol) are listed in parentheses.

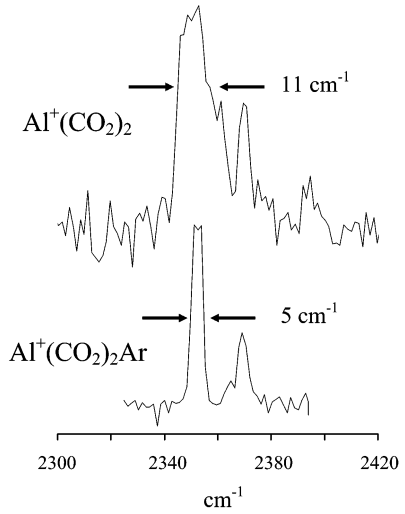

Figure 4. Infrared spectra of $Al^+(CO_2)_2$ in the upper trace and $Al^+(CO_2)_2Ar$ in the lower trace near the ν_3 of CO_2. Attaching argon reduces the line width from 11 to 5 cm^{-1}.

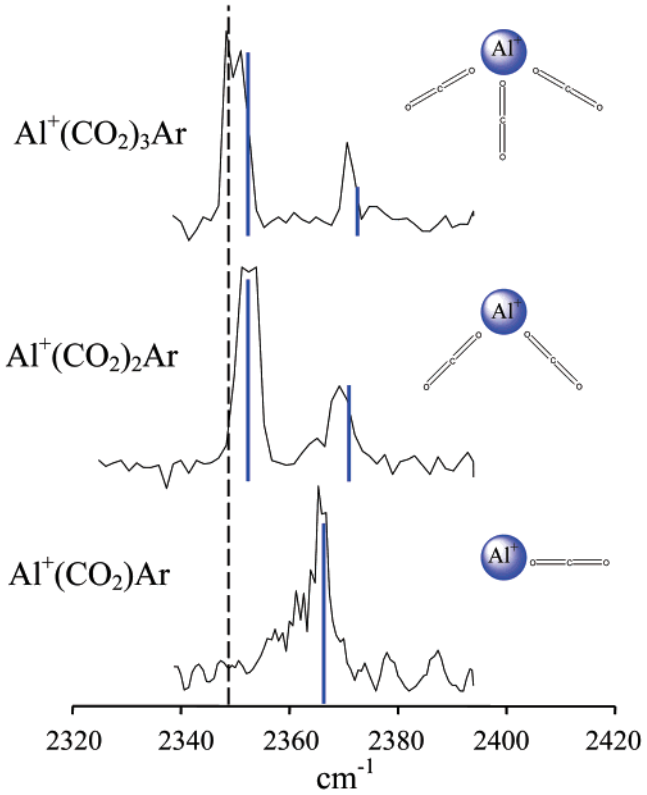

Figure 5. Infrared spectra of $Al^+(CO_2)_{1-3}Ar$ from 2300 to 2420 cm^{-1} compared to theoretically computed (B3LYP) frequencies for the structures indicated. The vertical dashed line indicates the vibrational frequency for free CO_2.

dissociation yield on resonance is about 20% for the $n = 2,3$ complexes and less than 10% for the $n = 1$ complex. Only one transition is observed for $Al^+(CO_2)Ar$ at 2366 ± 1 cm^{-1}, whereas two transitions are observed for $Al^+(CO_2)_2Ar$ at 2352 and 2369 ± 1 cm^{-1}. The line widths of these spectra are about 3−5 cm^{-1}, which are similar to those we observed previously for $Fe^+(CO_2)_nAr$ and $Mg^+(CO_2)_nAr$ complexes.[28,29] The lower binding energies and increased vibrational state densities produce higher fragmentation yields and sharp resonances for the argon-tagged complexes. Because of this, the spectra of the mixed clusters represent the best measurements possible for the smaller cluster sizes and these vibrational frequencies can be compared to the predictions of theory for the corresponding pure $Al^+(CO_2)_n$ complexes. The vertical blue bars added to Figure 5 show the positions and relative intensities of the vibrational bands calculated with the B3LYP functional for each of the lowest energy structures for the pure CO_2 complexes. As discussed below, the vibrations calculated for the pure $Al^+(CO_2)_n$ clusters are in nice agreement with those measured for the $Al^+(CO_2)_nAr$ species.

The linear structure for the $n = 1$ complex results in a single IR-active vibrational mode in the region of the asymmetric stretch calculated at 2367/2363 cm^{-1} (B3LYP/BP86). The spectrum for $Al^+(CO_2)Ar$ shows such a single feature at 2366 ± 1 cm^{-1}, consistent with the predicted linear configuration. This band is blue-shifted by 17 cm^{-1} from ν_3 of free CO_2. Similar blue-shifted vibrations were observed previously for Mg^+CO_2 and Fe^+CO_2 complexes.[28,29] As we have discussed before for these complexes,[28,29] the blue-shifted vibration results from increased repulsion on the inner potential wall caused by the presence of the metal ion. It is interesting to consider the magnitude of these spectral shifts, which should depend on the respective strengths of the metal−ligand interactions. Fe^+-CO_2 and Mg^+-CO_2 are both linear, and their ν_3 spectral shifts are +58 cm^{-1} and +32 cm^{-1} respectively.[28,29] The bond energies for these two complexes are comparable (about 15 kcal/mol).[10,11,29] However, the iron complex has a larger reduced mass and very different electronic structure than the magnesium complex, with perhaps some partial covalent character, and it is therefore not surprising that these two complexes differ in their vibrational frequencies. Although aluminum and magnesium have similar masses, and both are bound primarily by electrostatic interactions, the 17 cm^{-1} blue shift observed for Al^+CO_2 is considerably less than the 32 cm^{-1} shift for Mg^+-CO_2.[29] The same trend in vibrational shifts for these two complexes is predicted by theory.[29] The explanation for this trend is apparently the different binding energies for the two complexes. The Al^+CO_2 complex dissociation energy has not been measured. However, its calculated dissociation energy from this work (12.1 kcal/mol) can be compared to the value we calculated previously for Mg^+CO_2 (15.4 kcal/mol)[29] using about the same level of theory. The smaller binding energy for Al^+-CO_2 probably results from the combined effects of more effective ligand shielding by the Al^+ $3s^2$ electron cloud and a greater polarizability of the Mg^+ $3s^1$ valence electron cloud which allows it to distort more easily to accommodate ligands.

To explore the IR spectrum of the $n = 2$ complex, we must consider both in-phase and out-of-phase motions of the asymmetric stretch on the two CO_2 ligands. In a linear O═C═O−Al^+−O═C═O structure, the in-phase combination would not be IR active, but the out-of-phase combination would be. In a bent C_{2v} structure, such as the one calculated, both of these are IR active in the same way that the symmetric and asymmetric O−H stretches in water are both active. In the measured spectrum, two IR bands are observed for $Al^+(CO_2)_2$ at 2352 ± 1 and 2369 ± 1 cm^{-1}, consistent with the nonlinear structure calculated. From the calculations, we can assign the 2352 cm^{-1} band as the out-of-phase vibration and the 2369 cm^{-1} band as the in-phase vibration. In addition to the correct number of IR bands, both the blue shifts of these bands and their relative intensities match nicely with theory. These combined observations confirm that the theoretical structure is at least qualitatively correct.

In previous IR experiments on other metal ion-CO_2 complexes, we found that $Fe^+(CO_2)_2$ is linear with one IR-active mode in the asymmetric stretch region,[28] whereas $Mg^+(CO_2)_2$

is bent with two active modes here.[29] As discussed above, both the magnesium and aluminum complexes are bent because of the high polarizability of the valence 3*s* electrons. This effect is not operative in the case of iron, and the ligands are then situated to avoid each other more effectively in space. As we saw for the $n = 1$ complexes, the band positions for both $Al^+(CO_2)_2Ar$ and $Mg^+(CO_2)_2Ar$ (2368 and 2384 cm^{-1}) are blue shifted, but the blue shift is less for the aluminum complex. The $n = 2$ complex for aluminum is calculated to be bound less strongly than that of magnesium, and so lower vibrational frequencies are again understandable.

The $n = 3$ complex is predicted to have a C_{3v} trigonal pyramid structure. This configuration results from the same polarization effect of the metal ion valence electrons discussed above, which leads to same-side binding of the ligands. To consider the IR spectrum, we must again consider in-phase and out-of-phase combinations of the asymmetric stretch on three ligands. From this, it can be seen that a trigonal planar complex would have only one IR-active mode in this region (a degenerate 2+1 out-of-phase asymmetric stretch) whereas the nonplanar complex would have two IR-active modes (the degenerate out-of-phase asymmetric stretch and an in-phase asymmetric stretch). Surprisingly, we see *three* bands in the spectrum. There is a distinct blue-shifted peak at 2371 ± 1 cm^{-1} and a reproducible doublet at 2349/2351 cm^{-1}. Neither of the structures expected would have three IR-active bands, and therefore we must consider the possibility of some other structure or the possible presence of more than one isomer. The 2351 and 2371 bands are blue-shifted with respect to the free molecule, and these are in good agreement with the calculated positions of the out-of-phase and in-phase bands for the C_{3v} structure. As seen before for the $n = 1$ and 2 complexes, these bands for $Al^+(CO_2)_3Ar$ are lower in energy than the corresponding $Mg^+(CO_2)_3Ar$ modes (2364 and 2388 cm^{-1}) because of the weaker binding interaction with the aluminum cation. However, an additional band (the lower member of the doublet) is also seen in both the neat $Al^+(CO_2)_3$ complex and the tagged $Al^+(CO_2)_3Ar$ species that falls essentially on the position of the free CO_2 band. We have discussed before in our studies of other metal ion-CO_2 complexes how such a band can occur in these complexes.[28,29] In pure CO_2 clusters that only have binding of CO_2 with itself, the asymmetric stretch has about the same frequency as the free monomer.[60−66] Therefore, we have interpreted a band at the free-CO_2 frequency to indicate the presence of CO_2 molecules that are not attached to the metal ion and have no blue shift. A "2+1" isomer with one CO_2 not bound to metal might be expected to have a spectrum like that of the $n = 2$ species because there are two CO_2 molecules attached to the metal ion, and indeed the blue-shifted bands for both the $n = 2$ and n=3 species fall at nearly the same positions. Within the widths of these bands, it is possible that the spectrum for a 2+1 isomer would overlap that of the C_{3v} isomer. The spectrum could be consistent, therefore, with the presence of both the C_{3v} and the 2+1 isomers, or perhaps only the 2+1 isomer. In either case, it is clear that some significant number of CO_2 molecules prefer to bind externally to other CO_2 ligands and not to the metal at this very small cluster size. This is surprising, because the binding energy for the C_{3v} complex should be much greater than that for a 2+1 complex. The binding energies calculated (25.8 kcal/mol for the $n = 3$ C_{3v} structure versus 19.8 for the $n = 2$ C_{2v} structure) indicate an incremental $n = 2 \rightarrow n = 3$ bond energy of about 6 kcal/mol (2100 cm^{-1}) if the CO_2 attaches to the metal ion, whereas the bond energy for CO_2 with itself in a 2+1 complex is likely to be close to the $(CO_2)_2$ dimer binding of about 500 cm^{-1}.[53] However, it may be the dynamics of cluster growth rather than the energetics that lead to these isomers. If cluster growth occurs by sequential addition of CO_2 ligands, it is conceivable that the third ligand encounters the attractive part of the potential with CO_2 as it approaches the complex and binds initially to one of the ligands already present. If an activation energy is required to rearrange the system into the C_{3v} structure, then at the low temperature of this experiment some complexes would be able to rearrange and other might be trapped in the 2+1 "entrance channel." Although the quality of our spectra do not allow a definitive assignment, this growth mechanism is plausible and it is likely that the bands seen represent the presence of both the C_{3v} structure calculated to be most stable and the 2+1 isomeric species.

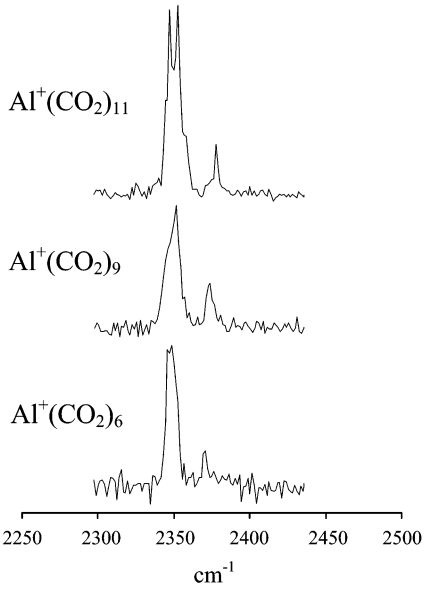

Figure 6. Infrared spectra of $Al^+(CO_2)_{6,9,11}$ depict a gradual blue-shift of the in-phase transition. A new feature appears in $Al^+(CO_2)_{11}$ to the blue of the out-of-phase stretch.

The larger $Al^+(CO_2)_n$ clusters ($n = 4-11$) could not be produced with attached argon in high enough intensity for REPD studies. The data we have for these systems therefore comes only from neat $Al^+(CO_2)_n$ complexes that photodissociate by the loss of CO_2. Each of the $n = 4-11$ species were scanned from 2100 to 3000 cm^{-1}. The spectra for the $n = 4,5$ species are shown in Figure 2, and the spectra for selected larger complexes ($n = 6,9,11$) are shown in Figure 6. It is interesting to note that the spectra for the $n = 4-8$ complexes are all almost identical, with two main transitions occurring at 2349 ± 1 cm^{-1} and 2371 ± 1 cm^{-1} for each of these systems. Whereas the $n = 3$ system had a closely spaced doublet near the free-CO_2 frequency, at $n = 4-8$ this is a single peak. However, this lower frequency band is broader in every spectrum than the weaker higher frequency band at 2371, suggesting that perhaps there are two peaks close together but not resolved. In our previous studies of other metal ion-CO_2 complexes, we saw bands assigned to the so-called "core" ligands (i.e., those attached to metal) that were more blue shifted away from the free CO_2 frequency.[28,29] As more CO_2 ligands were added to the cluster, an additional new band eventually grew in that was assigned to so-called "surface" ligands that were not attached to metal but instead were bound ligand-to-ligand.[28,29] A similar pattern in spectra might be expected here as these clusters grow in size. However, the blue shifts seen here for the these aluminum ion complexes are not very large. For example, the out-of-phase asymmetric stretch for the $n = 3$ complex in its C_{3v} structure

was calculated to be shifted by only 2 cm^{-1} from the free CO_2 frequency. Because of this small shift, it is likely that the same kind of out-of-phase vibration would be shifted even less in the complexes larger than $n = 3$, and then this band would essentially overlap with the vibrations of "surface" molecules when they begin to appear. This kind of overlap could explain the broad bands near 2349 cm^{-1} for the $n = 4-8$ complexes. However, because of this possible overlap problem, it is not possible to identify clearly when the "surface" molecules first begin to be formed. On the basis of our discussion above for the possible isomers at $n = 3$, and because of the broad bands seen, we suspect that some surface molecules are present for all of these complexes in the $n = 4-8$ size range. The same would of course also be true for larger complexes.

Beginning with the $n = 9$ complex, there are new gradual changes in these spectra. The 2349 band becomes broader and the band that was at 2371 in the $n = 4-8$ complexes shifts slightly to the blue. It appears at 2373 for the $n = 9$ complex, 2375 for $n = 10$ and 2378 for $n = 11$. Additionally, the spectrum for $Al^+(CO_2)_{11}$ shows that a doublet has appeared where the 2349 band was before, and the two members occur at 2347 and 2352 cm^{-1}. As we have discussed previously, there are two mechanisms that can cause ligand vibrations to shift to the blue in this size range. Core ligands can become confined by the growth of exterior layers, and this confinement causes an extra repulsion on the outer turning point of their vibrations. This causes a blue shift for the vibration in much the same way that binding to the metal ion does. The 2371 band in the small clusters is associated only with an in-phase motion of core ligands, and this must be the mechanism that causes it to shift toward the blue in the larger complexes. Surface ligands in the second layer around the metal (but not attached to the metal) can also blue shift for the same reason.[28,29] As the clusters grow larger, these molecules can also become confined by layers beyond the second one. This mechanism is only expected when the clusters have at least some molecules twice-removed from the metal ion, and it also occurs in larger pure $(CO_2)_n$ clusters.[61,65,66] In the case of iron-CO_2 complexes, a band caused by this effect first appeared at $n = 9$.[28] Considering this, the doublet near 2350 cm^{-1} in the $n = 11$ spectrum could arise from either of these two sources. It could represent molecules in the layer once-removed from the metal that are confined by additional molecules, or it could represent the vibration associated with the out-of-phase motion of core ligands that are blue-shifted by the additional confinement of outer layers. We are not able to distinguish between these two possibilities. However, it is interesting to note that the in-phase vibration near 2370 cm^{-1} shifts to the blue by about 6−7 cm^{-1} on going from $n = 6$ to $n = 11$, and the shift of the band near 2350 cm^{-1} is only about 2−3 cm^{-1}. In any event, it seems likely from all of these results that CO_2 molecules beyond those directly coordinated to Al^+ are probably present by the cluster size of $n = 4-8$, and definitely by the size of $n = 9$. Unfortunately, clusters here larger than $n = 11$ could not be studied in this work. The parent ion distribution drops off sharply after this size, and the ion density is then too low for these IRPD measurements.

In previous studies of the ionization behavior of neutral $Al(CO_2)_n$ complexes, we found evidence for an intracluster reaction producing $AlO(CO)(CO_2)_{n-1}$ products within the cluster.[42] The masses of these units are the same as those of the corresponding $Al(CO_2)_n$ complexes, and therefore mass spectrometry alone cannot distinguish between these two isomeric species. However, a reaction was inferred because the oxide/carbonyl species had higher ionization potentials due to the AlO moiety in the cluster. In the present study, we are examining aluminum metal *cations* clustering with CO_2, and it is interesting to consider if any such intracluster reaction occurs here. We have recently seen strong evidence for a similar metal ion insertion reaction with CO_2 in the case of $Ni^+(CO_2)_n$ complexes.[54] The evidence for this was a strongly shifted band occurring more than 100 cm^{-1} to the blue of the free CO_2 band, and this was assigned to arise from CO_2 molecules attached to the NiO^+ core, which has ion-pair (Ni^{2+}, O^-) bonding character. In the present aluminum system, there is no evidence for any strongly blue-shifted band, nor is there any evidence for a carbonyl stretch that might occur in these same clusters at lower frequencies in the 2000−2300 cm^{-1} region. We therefore conclude that ionized aluminum-CO_2 clusters do not undergo an intracluster reaction. In the future, we will investigate Al^+ clusters that grew first as neutrals and were then ionized subsequently to see if the IR spectra of these species indicate any reactions.

Conclusions

Infrared resonance-enhanced photodissociation spectra are reported for $Al^+(CO_2)_n$ complexes in the size range of $n = 1-11$. Fragmentation occurs by the loss of sequential CO_2 molecules. For the smaller cluster sizes, dissociation is more efficient in the argon-tagged complexes due to their lower binding energies and their higher vibrational density of states. No significant spectral shifts are observed for the argon-tagged complexes while the resulting line widths are considerably narrowed, making it possible to detect weak spectroscopic features. Density functional theory proposes linear, bent (C_{2v}), and pyramidal (C_{3v}) structures for the $n = 1-3$ complexes, respectively, and the experimentally observed vibrational spectra for the $n = 1$ and 2 complexes compare remarkably well to theoretical values. Binding of CO_2 ligands on the same side of the metal ion has been seen previously for magnesium complexes and attributed to the unusual polarizability of the valence $3s^1$ electron. The spectrum of the $n = 2$ complex here shows clearly that this same effect occurs for aluminum with its $3s^2$ valence configuration. Vibrational bands for ligands attached to the metal ion shift to higher frequencies compared to the asymmetric stretch in free CO_2. However, these blue shifts are less than those seen previously for magnesium ion or iron ion complexes with CO_2, presumably because the aluminum cation complexes are more weakly bound. Larger clusters have vibrational bands near the frequency of free CO_2, indicating the presence of molecules not attached to metal. The details of layer formation are not as clear here as they were for other cluster systems because the core ligand shifts are small and these bands overlap the free-CO_2 region. However, these data show that a significant number of externally bound ligands are already present at a cluster size of $n = 3$. All of these spectra are consistent with weak electrostatic bonding for aluminum cation complexes with CO_2. There is no evidence for any intracluster reactions that were suggested previously for neutral aluminum-CO_2 complexes.

Acknowledgment. We gratefully acknowledge support for this work from National Science Foundation (Duncan Grant No. CHE-0244143 and Schaefer Grant No. CHE-0136186).

References and Notes

(1) *Organometallic Ion Chemistry*; Freiser, B. S., Ed.; Kluwer: Dordrecht, 1996.

(2) *Gas-Phase Inorganic Chemistry*; Russell, D. H., Ed.; Plenum: New York, 1989.

(3) *Adv. Metal and Semiconductor Clusters*; Duncan, M. A., Ed., Elsevier Science: Amsterdam, 2001, Vol. 5.

(4) (a) Sodupe, M.; Bauschlicher, C. W., Jr. *Chem. Phys. Lett.* **1991**, *181*, 321. (b) Sodupe, M.; Bauschlicher, C. W., Jr.; Partridge, H. *Chem. Phys. Lett.* **1992**, *192*, 185. (c) Sodupe, M.; Branchadell, V.; Rosi, M.; Bauschlicher, C. W., Jr. *J. Phys. Chem. A.* **1997**, *101*, 7854. (d) Bauschlicher, C. W., Jr.; Partridge, H. *J. Phys. Chem.* **1991**, *95*, 9694. (e) Bauschlicher, C. W., Jr.; Sodupe, M.; Partridge, H. *J. Chem. Phys.* **1992**, *96*, 4453. (f) Partridge, H.; Bauschlicher, C. W., Jr.; Visscher, L. *Chem. Phys. Lett.* **1995**, *246*, 33.

(5) Watanabe, H.; Iwata, S.; Hashimoto, K.; Misaizu, F.; Fuke, K. *J. Am. Chem. Soc.* **1995**, *117*, 755. (b) Watanabe, H.; Iwata, S. *J. Phys. Chem. A* **1997**, *101*, 487. (c) Watanabe, H.; Iwata, S. *J. Chem. Phys.* **1998**, *108*, 10 078. (d) Fuke, K.; Hashimoto, K.; Iwata, S. *Adv. Chem. Phys.* **1999**, *110*, 431. (e) Watanabe, H.; Iwata, S. *J. Phys. Chem.* **1996**, *100*, 3377.

(6) (a) Yang, C. N.; Klippenstein, S. J. *J. Phys. Chem.* **1999**, *103*, 1094. (b) Klippenstein, S. J.; Yang, C. N. *Intl. J. Mass Spec.* **2000**, *201*, 253.

(7) Pandey, R.; Rao, B. K.; Jena, P.; Alvarez-Blanco, M. *J. Am. Chem. Soc.* **2001**, *123*, 3799.

(8) (a) Reinhard, B. M.; Niedner-Schatteburg, G. *J. Phys. Chem. A*, **2002**, *106*, 7988. (b) Reinhard, B. M.; Niedner-Schatteburg, G. *Phys. Chem. Chem. Phys.* **2002**, *4*, 1471. (c) Reinhard, B. M.; Niedner-Schatteburg, G. *J. Chem. Phys.* **2003**, *118*, 3571.

(9) (a) Stöckigt, D. *Chem. Phys. Lett.* **1996**, *250*, 387. (b) Stöckigt, D. *J. Phys. Chem. A.* **1997**, *101*, 3800.

(10) (a) Armentrout, P. B.; Baer, T. *J. Phys. Chem.* **1996**, *100*, 12 866. (b) Dalleska, N. F.; Honma, K.; Sunderlin, L. S.; Armentrout, P. B. *J. Am. Chem. Soc.* **1994**, *116*, 3519. (c) Meyer, F.; Khan, F. A.; Armentrout, P. B. *J. Am. Chem. Soc.* **1995**, *117*, 9740. (d) Rogers, M. T.; Armentrout, P. B. *Mass. Spectrom. Rev.* **2000**, *19*, 215. (e) Sievers, M. R.; Jarvis, L. M.; Armentrout, P. B. *J. Am. Chem. Soc.* **1998**, *120*, 1891. (f) Tjelta, B. L.; Armentrout, P. B. *J. Phys. Chem.* **1997**, *101*, 2064. (g) Tjelta, B. L.; Walter, D.; Armentrout, P. B. *Intl. J. Mass. Spectrom.* **2001**, *204*, 7.

(11) (a) Dunbar, R. C.; Klippenstein, S. J.; Hrusak, J.; Stöckigt, D.; Schwartz, H. *J. Am. Chem. Soc.* **1996**, *118*, 5277. (b) Petrie, S.; Dunbar, R. C. *J. Phys. Chem. A* **2000**, *104*, 4480.

(12) Bouchard, F.; Brenner, V.; Carra, C.; Hepburn, J. W.; Koyanagi, G. K.; McMahon, T. B.; Ohanessian, G.; Peschke, M. *J. Phys. Chem. A* **1997**, *101*, 5885.

(13) (a) Kemper, P. R.; Bushnell, J.; Bowers, M. T. *J. Phys. Chem. A* **1998**, *102*, 8590. (b) Kemper, P. R.; Weis, P.; Bowers, M. T.; Maitre, P. *J. Am. Chem. Soc.* **1998**, *120*, 13 494. (c) Weis, P.; Kemper, P. R.; Bowers, M. T. *J. Phys. Chem. A* **1997**, *101*, 2809. (d) Weis, P.; Kemper, P. R.; Bowers, M. T. *J. Phys. Chem. A* **1997**, *101*, 8207. (e) Zhang, Q.; Kemper, P. R.; Bowers, M. T. *Intl. J. Mass. Spectrom.* **2001**, *210*, 265. (f) Zhang, Q.; Kemper, P. R.; Shin, S. K.; Bowers, M. T. *Intl. J. Mass. Spectrom.* **2001**, *204*, 281.

(14) (a) Eller, K.; Schwarz, H. *Chem. Rev.* **1991**, *91*, 1121. (b) Hru×f0ák, J.; Stöckigt, D.; Schwarz, H. *Chem. Phys. Lett.* **1994**, *221*, 518.

(15) (a) Beyer, M. B. C.; Gorlitzer, H. W.; Schindler, T.; Achatz, U.; Albert, G.; Niedner-Schatteburg, G.; Bondybey, V. E. *J. Am. Chem. Soc.* **1996**, *118*, 7386. (b) Beyer, M. A.; Achatz, U.; Berg, C.; Joos, S.; Niedner-Schatteburg, G.; Bondybey, V. E. *J. Phys. Chem. A* **1999**, *103*, 671. (c) Bondybey, V. E.; Beyer, M.; Achatz, U.; Fox, B.; Niedner-Schatteburg, G. *Adv. Met. Semicond. Clusters*, **2001**, *5*, 295.

(16) Irion, M. P. *Intl. J. Mass Spectrom., & Ion Proc.* **1992**, *121*, 1.

(17) (a) Asher, R. L.; Bellert, D.; Buthelezi, T.; Weerasekera, G.; Brucat, P. J. *Chem. Phys. Lett.* **1994**, *228*, 390. (b) Asher, R. L.; Bellert, D.; Buthelezi, T.; Brucat, P. J. *Chem. Phys. Lett.* **1994**, *227*, 623. (c) Lessen, D. E.; Asher, R. L.; Brucat, P. J. *Adv. Met. Semicond. Clusters*, **1993**, *1*, 267.

(18) (a) Fuke, K.; Hashimoto, K.; Takasu, R. *Adv. Met. Semicond. Clusters*, **2001**, *5*, 1. (b) Sanekata, M.; Misaizu, F.; Fuke, K.; Iwata, S.; Hashimoto, K. *J. Am. Chem. Soc.* **1995**, *117*, 747. (c) Yoshida, S.; Okai, N.; Fuke, K. *Chem. Phys. Lett.* **2001**, 347, 93.

(19) (a) Shen, M. H.; Winniczek, J. W.; Farrar, J. M. *J. Phys. Chem.* **1987**, *91*, 6447. (b) Shen, M. H.; Farrar, J. M. *J. Phys. Chem.* **1989**, *93*, 4386. (c) Shen, M. H.; Farrar, J. M. *J. Chem. Phys.* **1991**, *94*, 3322. (d) Donnelly, S. G.; Farrar, J. M. *J. Chem. Phys.* **1993**, *98*, 5450.

(20) Kleiber, P. D. *Adv. Met. Semicond. Clusters* **2001**, *5*, 267.

(21) Velegrakis, M. *Adv. Met. Semicond. Clusters* **2001**, *5*, 227.

(22) (a) Faherty, K. P.; Thompson, C. J.; Aquirre, F.; Michne, J.; Metz, R. B. *J. Phys. Chem.* **2001**, *105*, 10 054. (b) Thompson, C. J.; Husband, J.; Aguirre, F.; Metz, R. B. *J. Phys. Chem. A.* **2000**, *104*, 8155. (c) Husband, J.; Aguirre, F.; Thompson, C. J.; Laperle, C. M.; Metz, R. B. *J. Phys. Chem. A.* **2000**, *104*, 2020.

(23) (a) Yeh, C. S.; Pilgrim, J. S.; Robbins, D. L.; Willey, K. F.; Duncan, M. A. *Int. Rev. Phys. Chem.* **1994**, *13*, 231. (b) Willey, K. F.; Yeh, C. S.; Robbins, D. L.; Duncan, M. A. *J. Chem. Phys.* **1993**, *98*, 1867. (c) Reddic, J. E.; Duncan, M. A. *J. Chem. Phys.* **1999**, *110*, 9948. (d) Pullins, S. H.; Scurlock, C. T.; Reddic, J. E.; Duncan, M. A. *J. Chem. Phys.* **1996**, *104*, 7518. (e) France, M. R.; Pullins, S. H.; Duncan, M. A. *J. Chem. Phys.* **1998**, *109*, 8842. (f) Duncan, M. A. *Annu. Rev. Phys. Chem.* **1997**, *48*, 69. (g) Duncan, M. A. *Int. J. Mass Spectrom.* **2000**, *200*, 545.

(24) (a) Willey, K. F.; Yeh, C. S.; Duncan, M. A. *Chem. Phys. Lett.* **1993**, *211*, 156. (b) Agreiter, J. K.; Knight, A. M.; Duncan, M. A. *Chem. Phys. Lett.* **1999**, *313*, 162.

(25) Wang, K.; Rodham, D. A.; McKoy, V.; Blake, G. A. *J. Chem. Phys.* **1998**, *108*, 4817.

(26) (a) Rothschopf, G. K.; Perkins, J. S.; Li, S.; Yang, D.-S. *J. Phys. Chem.* **2000**, *104*, 8178. (b) Yang, D.-S. *Adv. Met. Semicond. Clusters*, **2001**, *5*, 187. (c) Li, S.; Rothschopf, G. K.; Sohnlein, B. R.; Yang, D.-S. *J. Phys. Chem. A* **2002**, *106*, 6941. (d) Li, S.; Rothschopf, G. K.; Yang, D.-S. *J. Chem. Phys.* **2002**, *116*, 6589.

(27) (a) Cabarcos, O. M.; Weinheimer, C. J.; Lisy, J. M. *J. Chem. Phys.* **1999**, *110*, 8429. (b) Selegue, T. J.; Cabarcos, O. M.; Lisy, J. M. *J. Chem. Phys.* **1994**, *100*, 4790. (c) Weinheimer, C. J.; Lisy, J. M. *J. Phys. Chem.* **1996**, *100*, 15305. (d) Weinheimer, C. J.; Lisy, J. M. *Int. J. Mass Spectrom. Ion Processes* **1996**, *159*, 197. (e) Lisy, J. M. *Int. Rev. Phys. Chem.* **1997**, *16*, 267.

(28) (a) Gregoire, G.; Velasquez, J.; Duncan, M. A. *Chem. Phys. Lett.* **2001**, *349*, 451. (b) Gregoire, G.; Duncan, M. A. *J. Chem. Phys.* **2002**, *117*, 2120.

(29) Gregoire, G.; Brinkmann, N. R.; van Heijnsbergen, D.; Schaefer, H. F.; Duncan, M. A. *J. Phys. Chem. A* **2003**, *107*, 218.

(30) Walters, R. S.; Jaeger, T. D.; Duncan, M. A. *J. Phys. Chem. A* **2002**, *106*, 10 482.

(31) (a) van Heijnsbergen, D.; von Helden, G.; Meijer, G.; Maitre, P.; Duncan, M. A. *J. Am. Chem. Soc.* **2002**, *124*, 1562. (b) van Heijnsbergen, D.; Jaeger, T. D.; von Helden, G.; Meijer, G.; Duncan, M. A. *Chem. Phys. Lett.* **2002**, *364*, 345.

(32) Duncan, M. A. *Intl. Rev. Phys. Chem.* **2003**, in press.

(33) Lemaire, J.; Boissel, P.; Heninger, M.; Mauclaire, G.; Bellec, G.; Mestdagh, H.; Simon, A.; Le Caer, S.; Ortega, J. M.; Glotin, F.; Maitre, P. *Phys. Rev. Lett.* **2002**, *89*, 273 002.

(34) Panek, J.; Latajka, Z. *J. Phys. Chem. B* **1999**, *103*, 6845.

(35) Fangstrom, T.; Lunell, S.; Kasai, P.; Eriksson, L. *J. Phys. Chem.* **1998**, *102*, 1005.

(36) (a) Chaban, G.; Gordon, M. S. *J. Chem. Phys.* **1997**, *107*, 2160. (b) Chaban, G.; Gordon, M. S. *Chem. Phys. Lett.* **1997**, *278*, 195.

(37) Jursic, B. S. *Chem. Phys. Lett.* **1998**, *237*, 51.

(38) Sakai, S. *J. Phys. Chem.* **1993**, *97*, 8917.

(39) Heidecke, S. A.; Fu, Z.; Colt, J. R.; Morse, M. D. *J. Chem. Phys.* **1992**, *97*, 1692.

(40) (a) Yang, X.; Dagdigian, P. J.; Alexander, M. H. *J. Chem. Phys* **1998**, *108*, 3522. (b) Yang, X.; Dagdigian, P. J. *J. Chem. Phys.* **1998**, *109*, 8920.

(41) Misaizu, F.; Tsukamoto, K.; Sanekata, M.; Fuke, K. *Z. Phys. D.* **1993**, *26*, 177.

(42) Brock, L. R.; Duncan, M. A. *J. Phys. Chem.* **1995**, *99*, 16571.

(43) Lei, J.; Dagdigian, P. J. *Chem. Phys. Lett.* **1999**, *304*, 317.

(44) (a) Chen, J.; Wong, T. H.; Kleiber, P. D. *J. Chem. Phys.* **1999**, *110*, 11 798. (b) Chen, J.; Wong, T. H.; Kleiber, P. D. *Chem. Phys. Lett.* **1999**, *307*, 21. (c) Lu, W.-Y.; Liu, R.-G.; Wong, T.-H.; Chen, J.; Kleiber, P. D. *J. Phys. Chem. A.* **2002**, *106*, 725. (d) Lu, W. Y.; Acar, M.; Kleiber, P. D. *J. Chem. Phys.* **2002**, 116, 4847.

(45) Nakamoto, K. *Infrared and Raman Spectra of Inorganic and Coordinated Compounds*, 5th ed.; John Wiley: New York, 1997.

(46) Frisch, M. J.; Trucks, G. W.; Schlegel, H. B.; Gill, P. M. W.; Johnson, B. G.; Robb, M. A.; Cheeseman, J. R.; Keith, T.; Petersson, G. A.; Montgomery, J. A.; Raghavachari, K.; Al-Laham, M. A.; Zakrzewski, V. G.; Ortiz, J. V.; Foresman, J. B.; Cioslowski, J.; Stefanov, B. B.; Nanayakkhara, A.; Challacombe, M.; Peng, C. Y.; Ayala, P. Y.; Chen, W.; Wong, M. W.; Andres, J. L.; Replogle, E. S.; Gomperts, R.; Martin, R. L.; Fox, D. J.; Binkley, J. S.; Defrees, D. J.; Baker, J.; Stewart, J. P.; Head-Gordon, M.; Gonzalez, C.; Pople, J. A., GAUSSIAN 94, Revision C.3, Gaussian, Inc., Pittsburgh, PA, 1995.

(47) Becke, A. D. *J. Chem. Phys.* **1993**, *98*, 5648.

(48) Lee, C.; Yang, W.; Parr, R. G. *Phys. Rev. B* **1988**, *37*, 785.

(49) Becke, A. D. *Phys. Rev. A* **1988**, *98*, 3098.

(50) Perdew, J. P. *Phys. Rev. B* **1986**, *33*, 7046.

(51) Huzinaga, S. *J. Chem. Phys.* **1965**, *42*, 1293.

(52) Dunning, T. H. *J. Chem. Phys.* **1970**, *53*, 2823.

(53) Bukowski, R.; Sadlej, J.; Jeziorski, B.; Jankowski, P.; Szalewicz, K.; Kucharski, S. A.; Williams, H. A.; Rice, B. M. *J. Chem. Phys.* **1999**, *110*, 3785.

(54) Grieves, G. A.; Walters, R. S.; Walker, N. R.; Duncan, M. A., to be submitted.

(55) Alcami, M.; Mo, O.; Yanez, M. *Mass Spectrom. Rev.* **2001**, *20*, 195.

(56) (a) Okumura, M.; Yeh, L. I.; Lee, Y. T. *J. Chem. Phys.* **1985**, *83*, 3705. (b) Okumura, M.; Yeh, L. I.; Lee, Y. T. *J. Chem. Phys.* **1988**, *88*, 79. (c) Yeh, L. I.; Okumura, M.; Myers, J. D.; Price, J. M.; Lee, Y. T. *J. Chem. Phys.* **1989**, *91*, 7319.

(57) (a) Bieske, E. J.; Dopfer, O. *Chem. Rev.* **2000**, *100*, 3963. (b) Linnartz, H.; Verdes, D.; Maier, J. P. *Science* **2002**, *297*, 1166.

(58) (a) Menezes, W. J. C.; Knickelbein, M. B. *J. Chem. Phys.* **1993**, *98*, 1856. (b) Knickelbein, M. B.; Menezes, W. J. C. *Phys. Rev. Lett.* **1992**, *69*, 1046.

(59) (a) Ayotte, P.; Weddle, G. H.; Kim, J.; Johnson, M. A. *Chem. Phys.* **1998**, *239*, 485. (b) Ayotte, P.; Weddle, G. H.; Kim, J.; Johnson, M. A. *J. Am. Chem. Soc.* **1998**, *120*, 12361.

(60) Pino, T.; Boudin, N.; Brechnignac, P. *J. Chem. Phys.* **1999**, *111*, 7337.

(61) (a) Fraser, G. T.; Pine, A. S.; Lafferty, W. J.; Miller, R. E. *J. Chem. Phys.* **1987**, *87*, 1502. (b) Gough, T. E.; Miller, R. E.; Scoles, G. *J. Phys. Chem.* **1981**, *85*, 4041. (c) Jucks, K. W.; Huang, Z. S.; Dayton, D.; Miller, R. E.; Lafferty, W. *J. Chem. Phys.* **1987**, *86*, 4341. (d) Jucks, K. W.; Huang, Z. S.; Miller, R. E.; Fraser, G. T.; Pine, A. S.; Lafferty, W. J. *J. Chem. Phys.* **1988**, *88*, 2185.

(62) Muenter, J. S. *J. Chem. Phys.* **1991**, *94*, 2781.

(63) Walsh, M. A.; England, T. H.; Dyke, T. R.; Howard, B. J. *Chem. Phys. Lett.* **1985**, *120*, 313.

(64) Weida, M. J.; Spherhac, J. M.; Nesbitt, D. *J. Chem. Phys.* **1995**, *103*, 7685.

(65) Disselkamp, R.; Ewing, G. E. *J. Chem. Phys.* **1993**, *99*, 2439.

(66) Bonnamy, A.; Georges, R.; Benidar, A.; Boissoles, J.; Canosa, A.; Rowe, B. R. *J. Chem. Phys.* **2003**, *118*, 3612.